

A new dynamic discrete model of DC-DC PWM converters

Boris Axelrod, Yefim Berkovich*, and Adrian Ioinovici

*Department of Electrical and Electronics Engineering,
Holon Academic Institute of Technology, 52 Golomb St., Holon 58102, Israel*

** Corresponding author: berkovich@hait.ac.il*

Received 31 May 2005, accepted 20 July 2005

Abstract

A discrete dynamic models of open- and closed-loop DC-DC PWM buck- and boost-converters are discussed. The discrete model, as compared with a continuous one, has the following advantages: it provides more exact voltage and current values in view of their pulsating character, and is more adequate for the analysis of converters with digital control devices. The discrete model is obtained by s - and z -transformations of the basic equations set of the converter over a switching cycle. The theoretical results are confirmed by SPICE and Simulink simulation results and agree with the experimental results on a laboratory prototype.

1 Introduction

The continuous model is the most widely used in the analysis of dynamic and static modes of DC-DC PWM converters. The beginning of application of such model ascends to [1], with later applications extended to complex enough structures, for example in [2], and also to converters with soft switching [3]. The continuous model allows one to permit average values in dynamic and static modes, that is sufficient for a certain class of problems.

This approach, however, suffers from a number of the following main defects:

1. The continuous model does not give information about the change of the voltage and current instant values, as well as about their ripple.
2. Representation of DC-DC PWM converters with the help of the continuous model is badly combined with modern means of digital control and with the capability of construction of high-speed automatic control systems on their basis.
3. The usually used continuous linearized model generally cannot give understanding of such important modes as the period doubling and of the subsequent forming of chaotic modes [4].

As will be shown below, the proposed dynamic model completely eliminates two first defects. And though pulse linearized model is used, it, due to keeping its discrete character, can examine the unstable modes as the regimes with the consecutive period doubling.

DC-DC PWM converters form the electrical circuits with variable structure, each of which is described on a certain time interval by a set of differential equations. To get the complete solution of such circuit, the results of solution on separate intervals should be matched to get the general differential equation [5]. The characteristic feature of this paper is that the pulse model is obtained by s- and z-transformations of the complete initial equation set without its solution on separate intervals and without subsequent consecutive fitting of results and getting the final differential equation. Such a way is not only simpler, but also keeps a large clearness and is based only on some general characteristics of the circuit - such as the pulse and transitive characteristics.

The paper has the following structure. In Section 2 the general dynamic pulse model of the buck converter and its interpretation for an opened loop and a closed loop system is given. In Section 3 the construction of such model for boost converter in different modes is shown. In the last Section 4 the experimental test of the proposed theory is given.

2 Dynamic impulse model of buck converter

Fig. 1a shows the buck-converter, filter and load. The equation system describing this converter, can be written in the matrix form as

$$\begin{aligned}
\frac{dx}{dt} &= A_1x + B_1; \\
\frac{dy}{dt} &= A_2y + B_2; \\
d &= f(v_C),
\end{aligned} \tag{1}$$

where matrices

$$x^T = [x_1, x_2, \dots, x_n]; \quad (x_1 = i_0, x_n = v_o);$$

$$y^T = [y_1, y_2, \dots, y_n]; \quad (y_1 = k_o v_o, y_n = v_C)$$

and

$$B_1^T = [V_{in}d, 0, \dots, 0]; \quad B_2^T = [V_{ref}, 0, \dots, 0]$$

The equations are obtained using the notations of Fig. 2b, where d is the switching function of a buck converter. Let us write down the equation system (1) for the increments of all unknown parameters shown at Fig. 2:

$$\begin{aligned}
\frac{d\hat{x}}{dt} &= A_1\hat{x} + \hat{B}_1; \\
\frac{d\hat{y}}{dt} &= A_2\hat{y} + \hat{B}_2.
\end{aligned} \tag{2}$$

For linearizing the system (2), we will consider small enough values of increments. In this case, the increments \hat{d} can be replaced by the pulse function acting at the moment of the increments \hat{d} in view of reduction of its duration to a small enough value. The amplitude of pulse function should be equal to the duration of the increment \hat{d} . This transformation is shown in Fig. 2f. Using this transformation one gets for the matrix \hat{B}_1^T :

a) for the open loop system,

$$\hat{B}_1^T = \left[V_{in} \sum_{k=0}^n \delta(t - kT_s) \frac{\hat{V}_C}{V_{ramp}} T_s, 0, \dots, 0 \right], \tag{3}$$

b) for the closed loop system, $\hat{v}_C = f(t)$,

$$\hat{B}_1^T = \left[V_{in} \sum_{k=0}^n \delta(t - kT_s) \frac{\hat{v}_C(kT_s)}{V_{ramp}} T_s F, 0, \dots, 0 \right], \tag{4}$$

where F is the ripple factor.

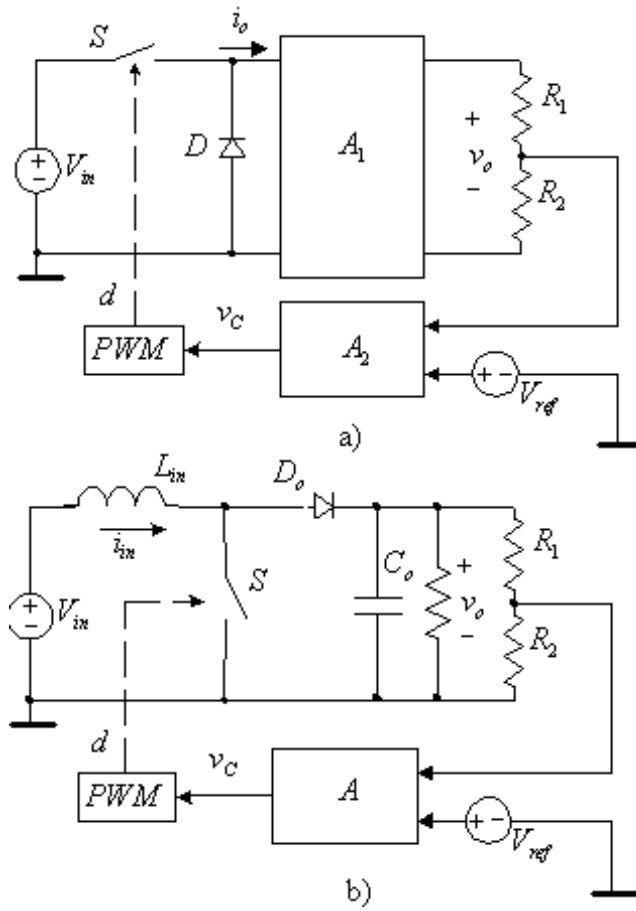


Figure 1: DC-DC PWM converters in a closed loop system. a) the buck converter, b) the boost converter.

The whole equation set has the form:

$$\hat{d} = f(\hat{v}_C). \quad (5)$$

The sense and meaning of the factor F will be explained in Section 2.

After the Laplace transform of (3), (4), one gets:

$$[Is - A_1] \hat{x}(s) = \hat{B}_1(s); \quad (6)$$

$$\hat{x}(s) = [Is - A_1]^{-1} \hat{B}_1(s),$$

where I is a unitary matrix.

The solution of system (6) relative to the parameters $\hat{x}_1 = \hat{i}_0$ and $\hat{x}_n = \hat{v}_o$ gives:

$$\hat{i}_0(s) = k_{in} \sum_{k=0}^{n-1} \frac{\left| \left[I s - A_1; \hat{B}_1(s)_1 \right] \right|}{\left| [I s - A_1] \right|}; \quad \hat{v}_o(s) = k_{in} \sum_{k=0}^{n-1} \frac{\left| \left[I s - A_1; \hat{B}_1(s)_n \right] \right|}{\left| [I s - A_1] \right|}, \quad (7)$$

After conversion of these expressions one gets

$$\begin{aligned} \hat{i}_o(s) &= k_{in} \sum_{k=0}^n X_{i_o}(s) e^{-kT_s} \hat{v}_C(kT_s); \\ \hat{v}_o(s) &= k_{in} \sum_{k=0}^n X_{V_o}(s) e^{-kT_s} \hat{v}_C(kT_s), \end{aligned} \quad (8)$$

where $X_{i_o}(s)$ and $X_{v_o}(s)$ are the Laplace transforms of the pulse characteristics of the general buck converter circuit at the closed switch condition relative to the input current i and output voltage v_o , respectively.

Going over the time domain

$$(X_{i_o}(s)e^{-kT_s} \rightarrow X_{i_o}(t - kT_s) \quad \text{and} \quad X_{v_o}(s)e^{-kT_s} \rightarrow X_{v_o}(t - kT_s)),$$

in discrete time points $t = nT_s$ and after z-transformation, one obtains z-images of required parameters:

$$\begin{aligned} \hat{i}_o(z) &= k_{in} \hat{v}_C(z) \cdot X_{i_o}^*(z); \\ \hat{v}_o(z) &= k_{in} \hat{v}_C(z) \cdot X_{V_o}^*(z). \end{aligned} \quad (9)$$

2.1 Open loop system

The transfer characteristics an "output current - control" and "output voltage - control" for the open loop system are:

$$\begin{aligned} G_{id}(z) &= k_{in} X_{i_o}^*(z); \\ G_{vd}(z) &= k_{in} X_{V_o}^*(z). \end{aligned} \quad (10a)$$

The transfer characteristics "output current - input voltage" and "output voltage - input voltage" for the open loop system are:

$$\begin{aligned} G_{iv}(z) &= k_c X_{i_o}^*(z); \\ G_{vv}(z) &= k_c X_{V_o}^*(z), \end{aligned} \quad (10b)$$

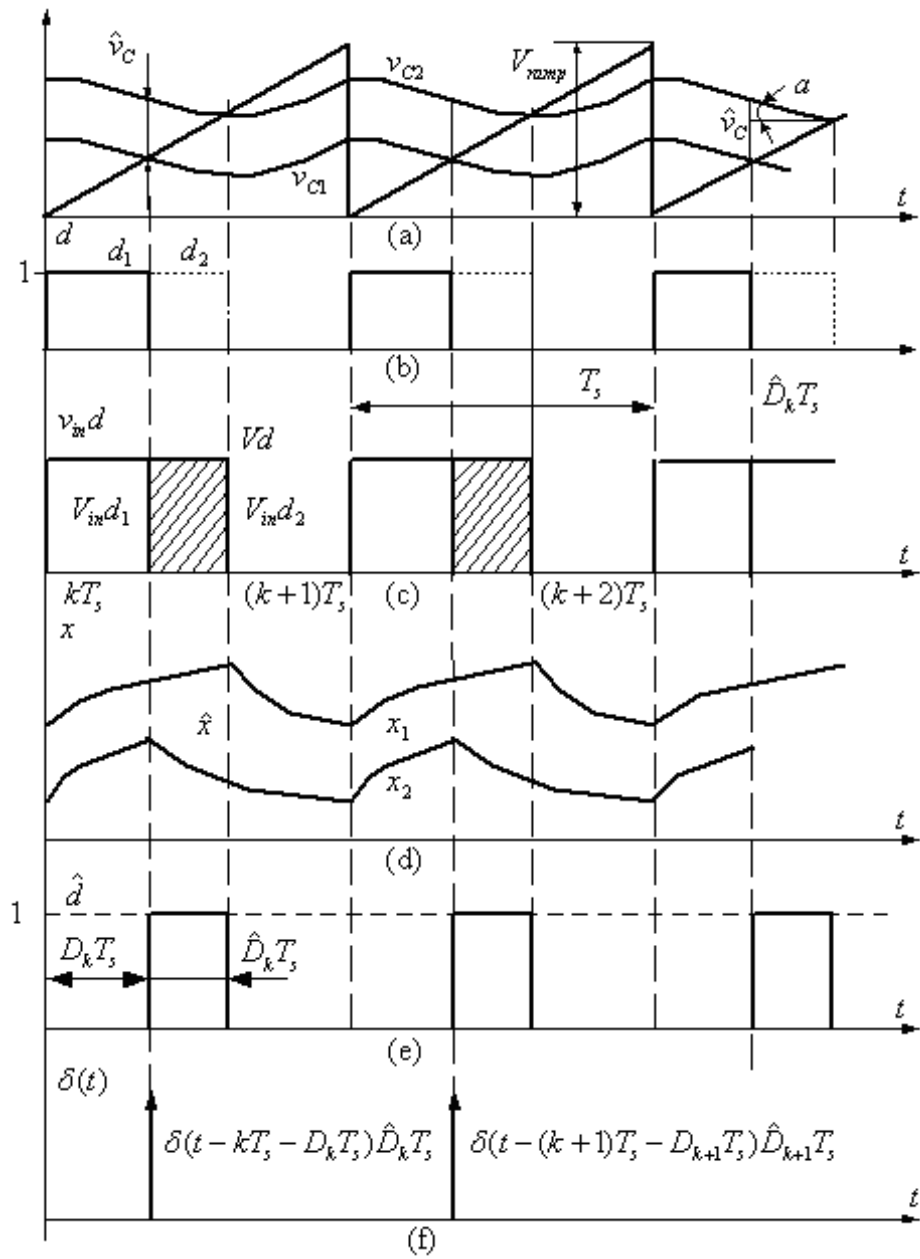


Figure 2: Main theoretical waveforms of the buck converter circuit.

where

$$k_C = \frac{V_C F T_s}{V_{ramp}}.$$

The adequacy of use of a pulse sequence function for the description of transients is checked up with the help of simulation programs Matlab-Simulink for the model constructed for the following parameters of buck converter: $V_{in} = 24V$, $L_o = 100\mu H$, $C_o = 5\mu F$, $R_o = 2.9\Omega$, $R_{in} = 0.1\Omega$, $f = 50kHz$, $V_{ramp} = 5V$, $D = 0.5$. In Fig. 3 the circuit of model corresponding to (8) is shown. For its construction it is necessary to know only Laplace transforms of the pulse characteristics

$$X_{i_o}(s) = \frac{1}{L_o} \frac{s + 2\Delta_1}{s^2 + 2\Delta s + \omega_o^2}, X_{V_o}(s) = \frac{1}{L_o C_o} \frac{1}{s^2 + 2\Delta s + \omega_o^2}.$$

where

$$\Delta = \frac{1}{2R_o C_o} + \frac{R_{in}}{2L_o}; \Delta_1 = \frac{1}{2R_o C_o}; \omega_o^2 = \left(1 + \frac{R_{in}}{R_o}\right) \frac{1}{L_o C_o}.$$

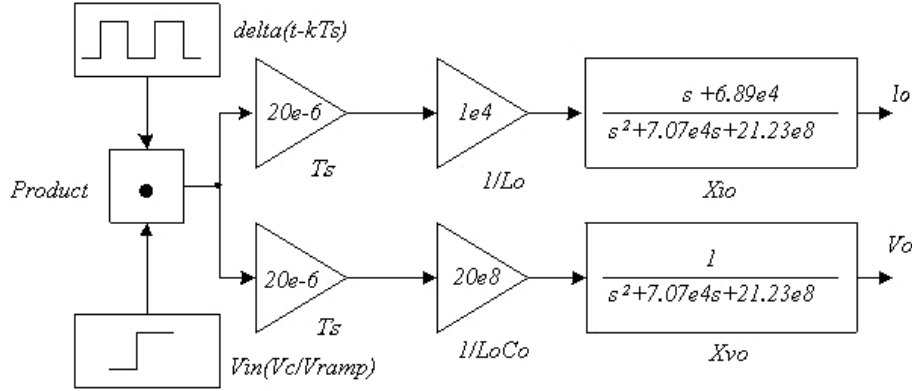


Figure 3: Simulation Matlab-Simulink s-model for the buck converter in an open loop system.

The curves of the output voltage and current response to a jump of the input voltage from zero to V_{in} are given at Fig. 4a for the model of Fig. 3 (s -transformations) and according to (10b) (z -transformation), where

$$X_{i_o}^*(z) = \frac{\omega_o - 2\Delta_2}{\omega L_o} \frac{z^2 \sin \phi + z e^{-\bar{\Delta}} (\sin(\bar{\omega} - \phi) - \sin \bar{\omega})}{z^2 - 2z e^{-\bar{\Delta}} \cos \bar{\omega} + e^{-2\bar{\Delta}}},$$

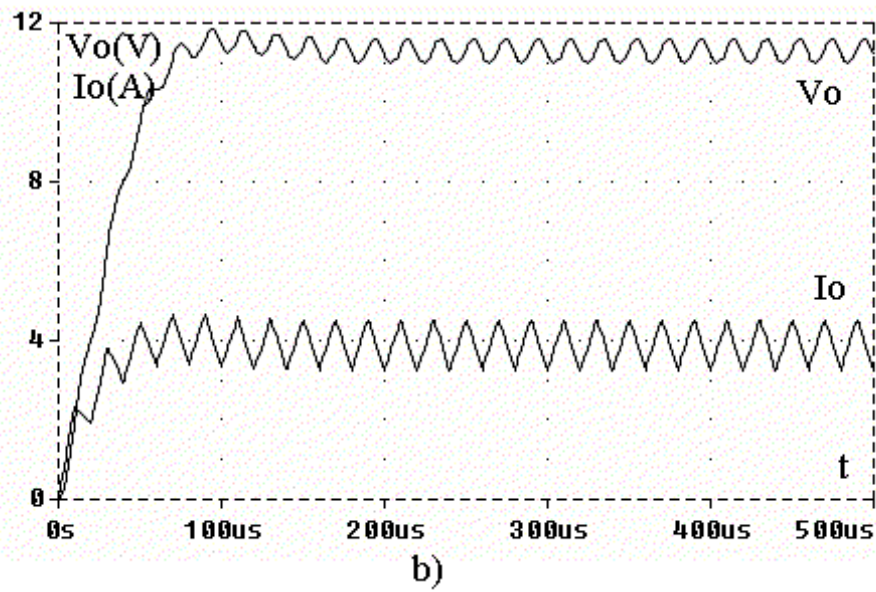
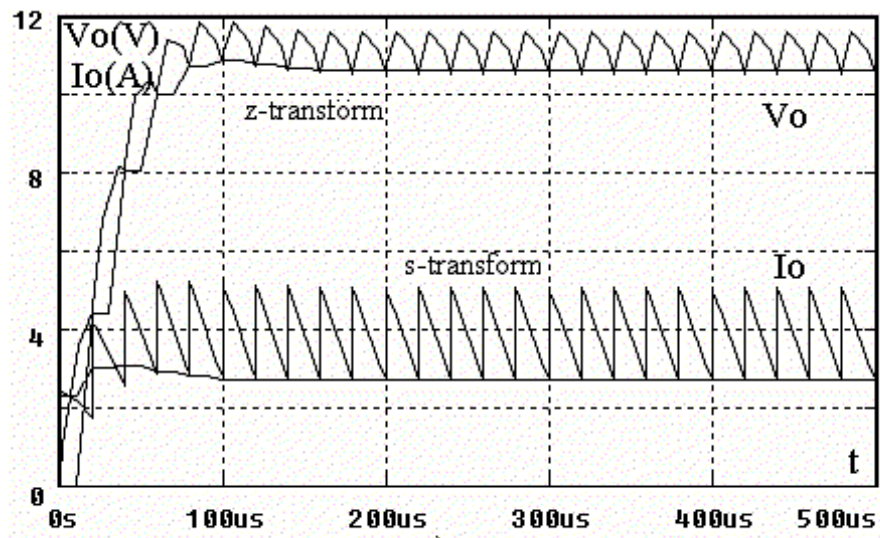


Figure 4: Simulation results of a step-up transient for the buck converter in an open loop system. a) Matlab-Simulink s-model, b) PSPICE simulation.

and

$$\Delta_2 = \Delta - \Delta_1, \bar{\Delta} = \Delta \cdot T_s, \omega = \sqrt{\omega_o^2 - \Delta^2}, \bar{\omega} = \omega \cdot T_s, \quad tg\phi = \frac{\omega}{\Delta}.$$

The results of simulation of the same transient processes in PSPICE are given at Fig. 4b.

2.2 Closed loop system

$$\hat{v}_C(s) = \left(\frac{\hat{v}_{ref}(s)}{s} - k_o \hat{v}_o(s) \right) \cdot G(s). \quad (11)$$

Going over time domain and taking into account the value of $\hat{v}_o(s)$ from (8), one gets

$$\hat{v}_C(t) = G_1(t) \hat{v}_{ref} - k_o k_{in} \sum_{k=0}^{n-1} \hat{v}_C(kT_s) \cdot G_2(t - kT_s), \quad (12)$$

where

$$G_1(t) \div G(s) \frac{1}{s}; \quad G_2(t) \div G(s) X_{V_o}(s).$$

Passing to z -transform, one gets for discrete moments $t = nT_s$

$$\hat{v}_C(z) = G_1^*(z) \hat{V}_{ref} - k_o k_{in} \hat{v}_C(z) G_2^*(z), \quad (13a)$$

from which

$$\hat{v}_C(z) = \hat{V}_{ref} \frac{G_1^*(z)}{1 + k_o k_{in} G_2^*(z)} \quad (13b)$$

and

$$\hat{v}_o(z) = \hat{V}_{ref} \frac{k_{in} G_1^*(z) X_{V_o}^*(z)}{1 + k_o k_{in} G_2^*(z)}. \quad (13c)$$

Expressions (13b) and (13c) for the closed loop system in z -plane can be obtained directly: $X_{V_o}^*(z)$ is the transfer function of the closed loop system, $G_1^*(z)$ is the transfer function of the regulator. So:

$$\hat{v}_C(z) = \hat{V}_{ref} \frac{G_1^*(z)}{1 + k_o k_{in} G_1^*(z) X_{V_o}^*(z)} \quad (13d)$$

and

$$\hat{v}_o(z) = \hat{V}_{ref} \frac{k_{in} G_1^*(z) X_{V_o}^*(z)}{1 + k_o k_{in} G_1^*(z) X_{V_o}^*(z)}.$$

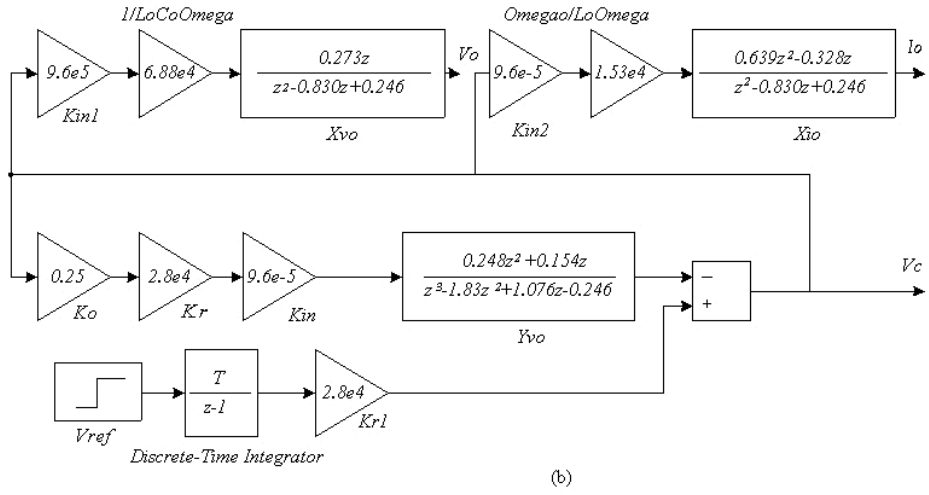
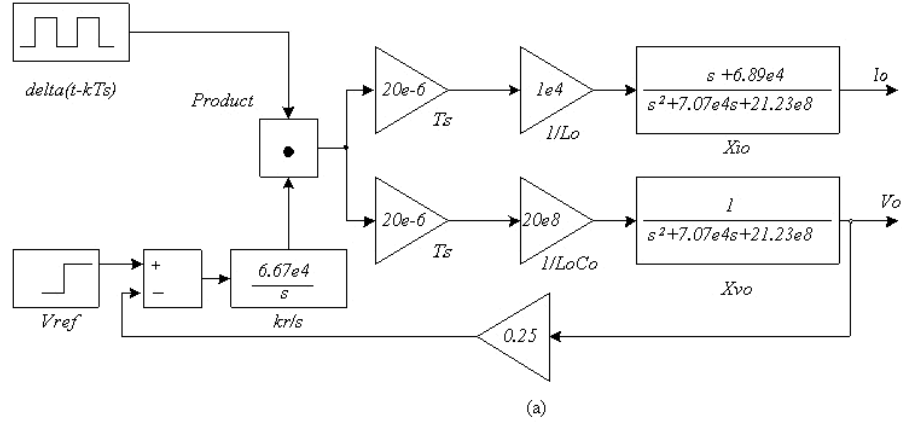


Figure 5: Simulation Matlab-Simulink s -model (a) and z -model (b) for the buck converter in a closed loop system.

Factor F , in (4), reflects the character of pulsations of the output voltage in the closed loop system. The meaning of F and its definition are explained in Fig. 2a. It can be seen that $\hat{V}_C = \Delta t \cdot \tan \alpha_1 - \Delta t \cdot \tan \alpha_2$, from which

$$\Delta t = \frac{\hat{V}_C}{\tan \alpha_1 - \tan \alpha_2} \quad (14a)$$

and, further, taking into account that $\tan \alpha_1 = \frac{1}{T_s}$ and also that $\tan \alpha_2 = \left[\frac{dV_C}{dt} \right]_{nT-0}$, one gets

$$\Delta t = \frac{\hat{V}_C}{\frac{1}{T_s} - \left[\frac{dV_C}{dt} \right]_{nT-0}} = \frac{\hat{V}_C T_s}{1 - T_s \left[\frac{dV_C}{dt} \right]_{nT-0}} = F T_s \hat{V}_C, \quad (14b)$$

where

$$F = \frac{1}{1 - T_s \left[\frac{dV_C}{dt} \right]_{nT-0}}. \quad (14c)$$

As it can be seen, $F \leq 1$, i. e., the total gain factor is reduced. Factor F is determined for different loads, in particular for the $L_o - R_o$ - load one gets

$$F^{-1} = 1 + \frac{T_s}{T_o} \cdot \frac{e^{-\frac{T_s}{T_o} \gamma_o} - e^{-\frac{T_s}{T_o}}}{1 - e^{-\frac{T_s}{T_o}}} \quad (15)$$

where $T_o = \frac{L_o}{R_o}$.

Accepting $G_1^*(z) = k_r \frac{T_s}{z-1}$ ($G_1^*(z)$ is a discrete integrator, $k_r = 1/T_c$), one gets

$$\hat{v}_C(z) = \frac{z \cdot \hat{V}_{ref}}{z-1} \cdot \frac{\frac{k_r \cdot T_s}{z-1}}{1 + k_o k_{in} k_r \frac{T_s}{z-1} X_{V_o}^*(z)}. \quad (16a)$$

Now, based on (16a)

$$\hat{v}_o(z) = \frac{z \cdot \hat{V}_{ref}}{z-1} \cdot \frac{\frac{k_r \cdot T_s}{z-1} k_{in} X_{V_o}^*(z)}{1 + k_o k_{in} k_r \frac{T_s}{z-1} X_{V_o}^*(z)}. \quad (16b)$$

The Matlab-Simulink model of the closed loop system is shown in Fig. 5a. The model is obtained based on the model Fig. 3 and takes into account (8), (13b), (13c) for the buck converter from Section 2 and $G_2(s) = \frac{1}{sT_C}$ for the regulator, where $T_C = 15\mu s$ and $k_o = 0.25$, $V_{ref} = 3V$. The transient curves calculated in this model are shown in Fig. 6a. The model of the same closed loop system in a z -plane is given in Fig. 5b, and corresponding transient curves - in Fig. 6a. The results of PSPICE-modeling are given for comparison in Fig. 6b.

From expressions (13c) and (13d) one can get the characteristic equation of the closed loop system

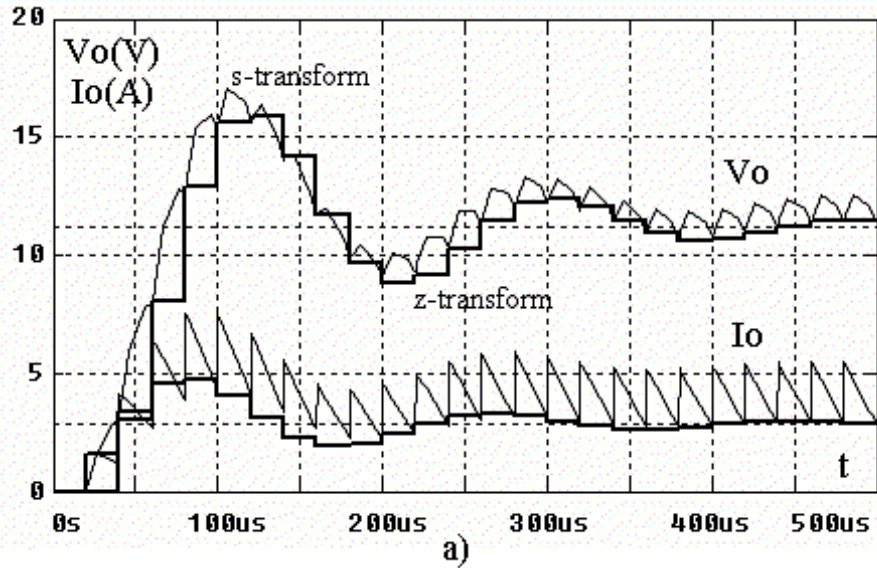


Figure 6: Simulation results of a step-up transient process for the buck converter in a closed loop system. a) Matlab-Simulink s - and z -models, b) PSPICE simulation.

$$\begin{aligned} 1 + k_o k_{in} G_2^*(z) &= 0, \\ 1 + k_o k_{in} G_1^*(z) X_{V_o}^*(z) &= 0. \end{aligned} \quad (17)$$

On the basis of these equations one can get the stability condition of the system: the system is stable if $|z| < 1$. Root locus for $F(z, K) = 1 + K k_o k_{in} G_1^*(z) X_{V_o}^*(z)$ for the buck converter from Section 2 and for the regulator $G_2(s) = \frac{1}{s T_C}$, where $T_C = 36 \mu s$ and $k_o = 0.25, V_{ref} = 3V$, are given in Fig. 7. The analysis shows that stability of the system is provided for $K \leq 2$.

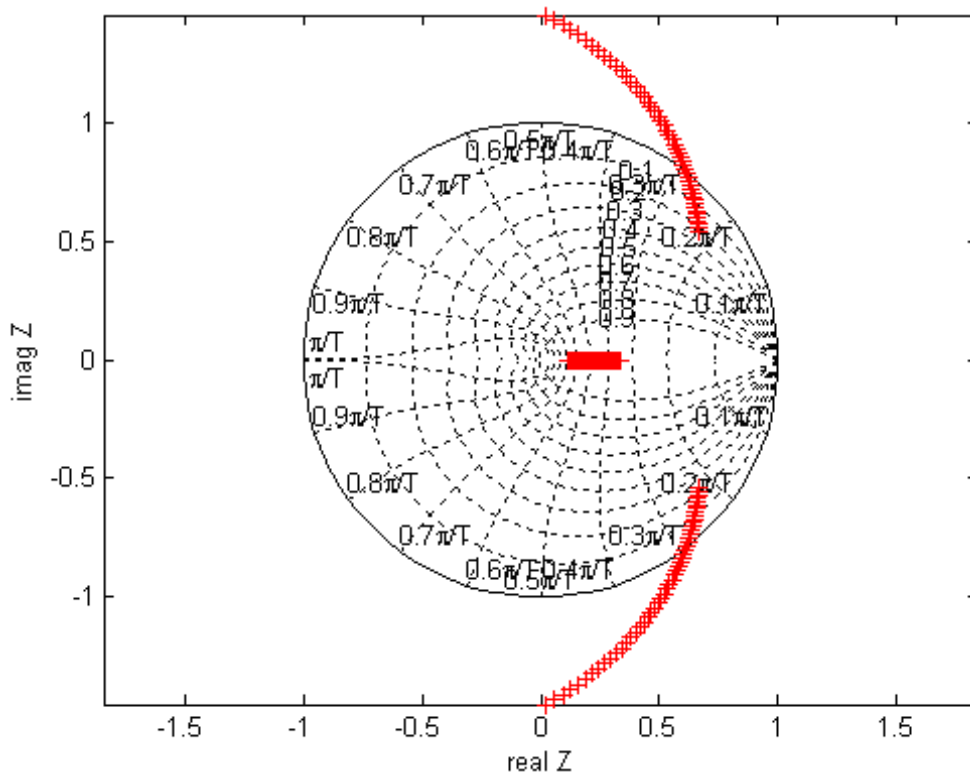


Figure 7: Locus of the roots for z-models of the buck converter.

3 Dynamic impulse model of boost converter

The scheme of the boost converter with the closed loop system of regulation is presented in Fig. 1b. Taking into account notations of Fig. 1b and Fig. 8a,b, the system of equations for the open loop system can be written as

$$\begin{aligned} L_{in} \frac{di_{in}}{dt} + v_o d_1 &= V_{in}; \\ C_o \frac{dv_o}{dt} + \frac{v_o}{R_o} &= i_{in} d_1. \end{aligned} \quad (18)$$

3.1 Open loop system ($D=\text{const}$)

For changes of only input voltage, the equations for increments are:

$$\begin{aligned} L_{in} \frac{d\hat{i}_{in}}{dt} + \hat{v}_o d_1 &= \hat{V}_{in}; \\ C_o \frac{d\hat{v}_o}{dt} + \frac{\hat{v}_o}{R_o} &= \hat{i}_{in} d_1. \end{aligned} \quad (19)$$

Replacing the increments by the equivalent pulse functions, one gets

$$\begin{aligned} L_{in} \frac{d\hat{i}_{in}}{dt} &= \hat{V}_{in} T_s \sum_{k=0}^n \delta(t - kT_s) - D_1 T_s \sum_{k=0}^n \hat{v}_{o,k}^* \delta(t - kT_s - DT_s); \\ C_o \frac{d\hat{v}_o}{dt} + \hat{v}_o &= D_1 T_s \sum_{k=0}^n \hat{i}_{in,k}^* \delta(t - kT_s - DT_s), \end{aligned} \quad (20)$$

where $\hat{i}_{in,k}$, $\hat{v}_{o,k}$ are the instantaneous values of the current \hat{i}_{in} and voltage \hat{v}_o at the moments $t = kT_s$, and $\hat{i}_{in,k}^*$ and $\hat{v}_{o,k}^*$ are the values of these parameters at the moments $t = kT_s + DT_s$.

Caring out the same sequence of operations as in the case of the buck-converter, i. e., producing the Laplace transformation and replacing it by the z -transformation, one gets

$$\begin{aligned} \hat{i}_{in}(z) + \frac{D_1 T_s}{L_{in}} \frac{z}{z-1} \hat{v}_o^*(z) &= \hat{V}_{in} \frac{T_s}{L_{in}} \frac{z^2}{(z-1)^2}; \\ -\frac{D_1 T_s}{C_o} \frac{ze^{-\Delta D}}{z - e^{-\Delta}} \hat{i}_{in}^*(z) + \hat{v}_o(z) &= 0, \end{aligned} \quad (21)$$

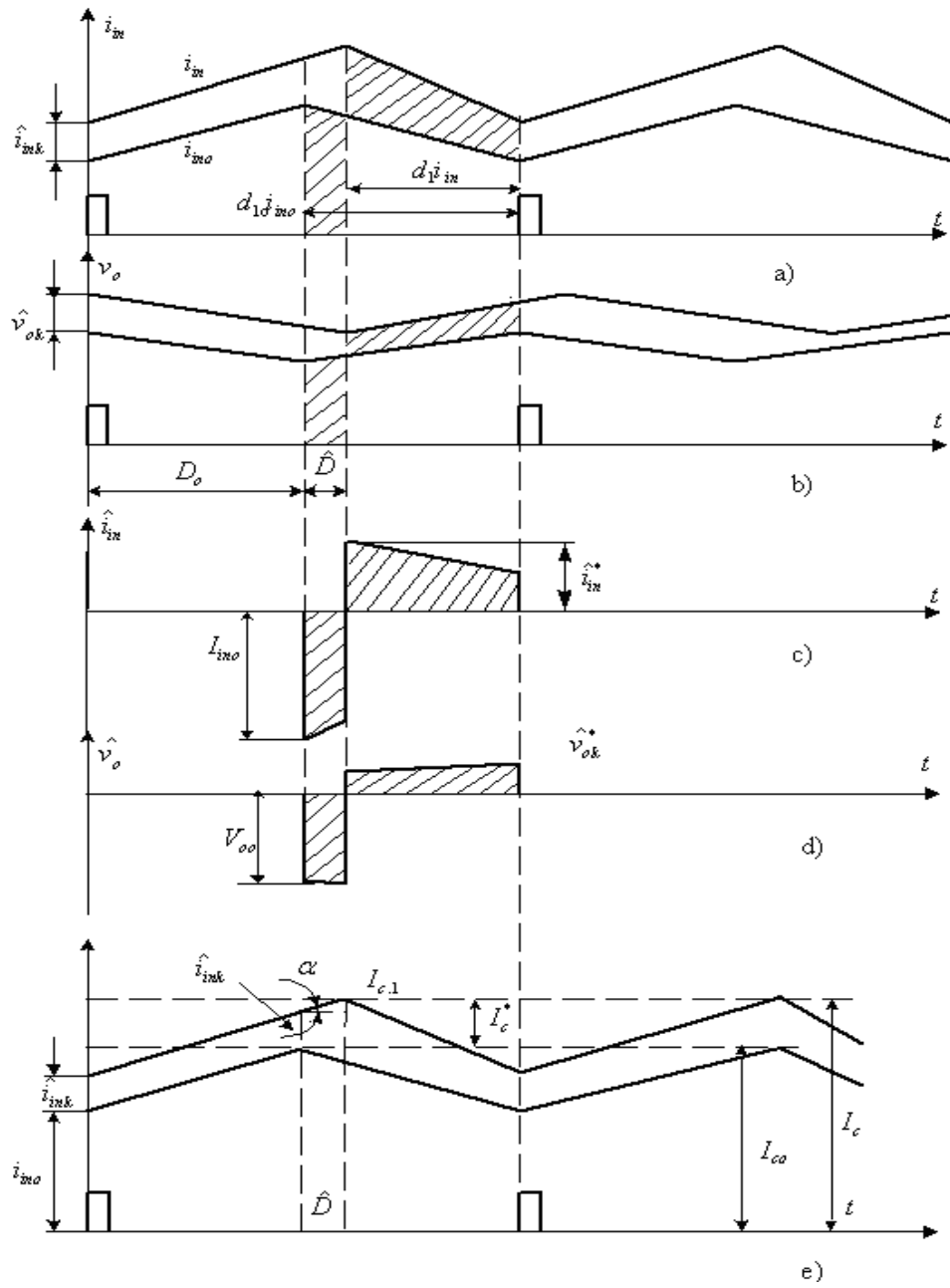


Figure 8: Main theoretical waveforms of the boost converter circuit.

where $\Delta = \frac{T_s}{R_o C_o}$.

Let us express the values of parameters marked by the symbol (*) with the aid of the parameters $\hat{i}_{in,k}(z)$ and $\hat{v}_{o,k}(z)$:

$$\begin{aligned} \hat{i}_{in}^*(z) &= \hat{i}_{in}(z) + \hat{V}_{in}(z) \frac{DT_s}{L_{in}}; \\ \hat{v}_o^*(z) &= \hat{v}_o(z) e^{-\Delta D}. \end{aligned} \quad (22)$$

This results in the following set of equations:

$$\begin{aligned} \hat{i}_{in}(z) + a_V(z) \hat{v}_o(z) &= \hat{V}_{in} \frac{T_s}{L_{in}} \frac{z^2}{(z-1)^2}; \\ -a_i(z) \hat{i}_{in}(z) + \hat{v}_o(z) &= \hat{V}_{in} \frac{DT_s}{L_{in}} a_i(z) \frac{z}{z-1}, \end{aligned} \quad (23)$$

where

$$a_V(z) = \frac{D_1 T_s}{L_{in}} \frac{z e^{-\Delta D}}{z-1}; \quad a_i(z) = \frac{D_1 T_s}{C_o} \frac{z e^{-\Delta D}}{z - e^{-\Delta}}.$$

Based on (23), one gets for the boost converter

$$\begin{aligned} G_{iv}(z) &= \frac{T_s}{L_{in}} \frac{b_{2i} z^2 + b_{1i} z}{a_2 z^2 + a_1 z + a_0}; \\ G_{vv}(z) &= \frac{D_1 T_s^2 e^{-\Delta D}}{L_{in} C_o} \frac{b_{2v} z^2 + b_{1v} z}{a_2 z^2 + a_1 z + a_0}, \end{aligned} \quad (24)$$

where

$$\begin{aligned} a_0 &= e^{-\Delta}; \quad a_1 = -(1 + e^{-\Delta}); \quad a_2 = 1 + \frac{D_1^2 T_s^2}{L_{in} C_o} e^{-2\Delta D}; \\ b_{2i} &= 1; \quad b_{1i} = -(e^{-\Delta} + \frac{D_1^2 T_s^2}{L_{in} C_o} D e^{-2\Delta D}); \\ b_{2v} &= (1 + D) \frac{D_1 T_s^2}{L_{in} C_o} e^{-\Delta D}; \quad b_{1v} = -\frac{D_1 T_s^2}{L_{in} C_o} D e^{-\Delta D}. \end{aligned}$$

Fig. 9 shows the schemes of the Simulink-models, which are based on the direct simulation (20) and on the z -transformation (24). Fig. 10a shows the results of simulation of the starting process of the boost-converter with the following parameters:

$$V_{in} = 24V; \quad L_{in} = 400\mu H; \quad C_o = 20\mu F; \quad R_o = 10\Omega; \quad f_s = 50kHz; \quad D = 0.5.$$

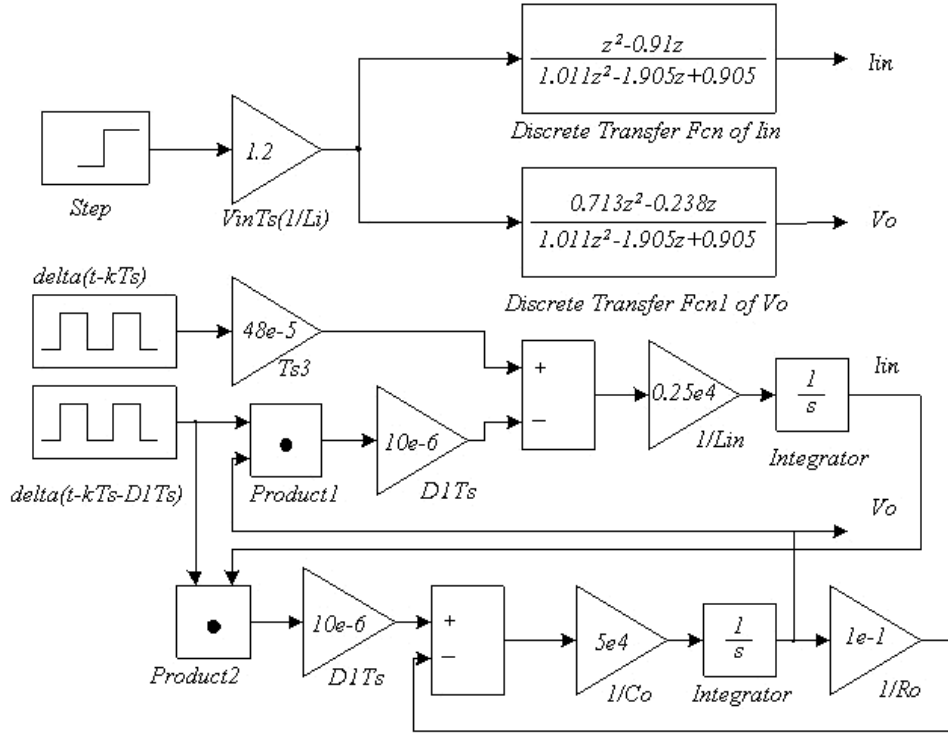


Figure 9: Simulation Matlab-Simulink s - and z -models for the boost converter in an open loop system.

3.2 Open loop system ($V_{in}=\text{const}$)

Let us consider construction of a pulse model of the boost-converter at change of its duty cycle. Fig. 8c,d shows the graphics of current i_{in} and voltage v_o for the change of the duty cycle from its initial value (marked by index “0”) to its final value for a general change of duty cycle \hat{D} . Based on the notations of Fig. 8c,d , we can obtain the following set of equations:

$$L_{in} \frac{d\hat{i}_{in}}{dt} + (d_1 \hat{v}_o - d_{10} V_{oo}) = 0; \quad (25a)$$

$$C_o \frac{d\hat{v}_o}{dt} + \frac{\hat{v}_o}{R_o} = (d_1 i_{in} - d_{10} I_{ino}).$$

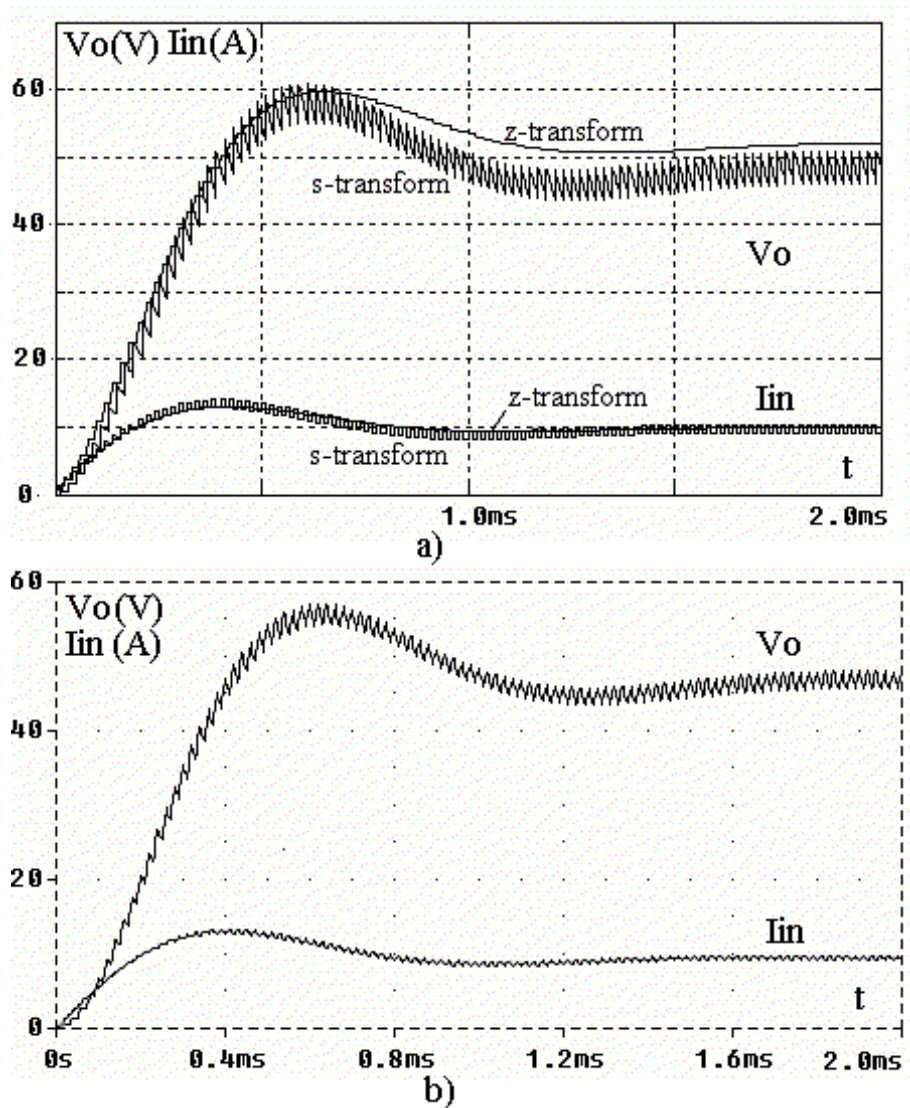


Figure 10: Simulation results of a step-up transient process for the boost converter in an open loop system ($D=\text{const}$). a) Matlab-Simulink s - and z -models, b) PSPICE simulation.

After transition to pulse functions and substitution of the right-hand term values we have:

$$\begin{aligned} L_{in} \frac{d\hat{i}_{in}}{dt} &= V_{oo}T_s \sum_{k=0}^n \hat{D}_k \delta(t - kT_s - DT_s) - D_1T_s \sum_{k=0}^n \hat{v}_{o.k}^* \delta(t - kT_s - DT_s); \\ C_o \frac{d\hat{v}_o}{dt} + \hat{v}_o &= D_1T_s \sum_{k=0}^n \hat{i}_{in.k}^* \delta(t - kT_s - DT_s) - I_{ino}T_s \sum_{k=0}^n \hat{D}_k \delta(t - kT_s - DT_s) \end{aligned} \quad (25b)$$

Now, based on Fig. 8c,d, we can write down the increments of all values and after that perform the s - and z -transformations. As a result, we obtain the following set of equations:

$$\begin{aligned} \hat{i}_{in}(z) + a_V(z)\hat{v}_o(z) &= \hat{D} \frac{V_{oo}T_s}{L_{in}} \left(\frac{z}{z-1} \right)^2; \\ -a_i(z)\hat{i}_{in}(z) + \hat{v}_o(z) &= \hat{D} \left(-\frac{I_{ino}}{D_1} + \frac{V_{in}T_s}{L_{in}} \right) a_i(z) \frac{z}{z-1}, \end{aligned} \quad (26)$$

from which

$$\begin{aligned} G_{id}(z) &= \frac{V_{oo}T_s}{L_{in}} \frac{b_{2iD}z^2 + b_{1iD}z}{a_2z^2 + a_1z + a_0}; \\ G_{vd}(z) &= \frac{V_{oo}T_s}{L_{in}} \frac{b_{2vD}z^2 + b_{1vD}z}{a_2z^2 + a_1z + a_0}, \end{aligned} \quad (27)$$

where

$$b_{2iD} = \left(1 - g \frac{D_1^2 T_s^2}{L_{in} C_o} e^{-2\Delta D} \right); \quad b_{1iD} = -e^{-\Delta}; \quad g = \frac{V_{in}}{V_{oo}} - \frac{I_{ino} L_{in}}{V_{oo} D_1 T_s};$$

and

$$b_{2vD} = \frac{D_1 T_s}{C_o} (1 + g) e^{-\Delta D}; \quad b_{1vD} = -\frac{D_1 T_s}{C_o} g e^{-\Delta D}.$$

The Simulink simulation results for a pulse model are presented in Fig. 11. The values of parameters are the same as in the previous case for $\hat{D} = 0.1$.

3.3 Pulse model of the boost converter in CCM

In the current control mode, the voltage and current changes in the boost converter are determined by the given change of current from its initial level I_{Co} to the level I_C (Fig. 8e). This results in a change in \hat{D} :

$$\hat{D} = (\hat{I}_C - \hat{i}_{in.k}) \cot \alpha, \quad (28)$$

where $\hat{I}_C = I_C - I_{Co}$; $\cot \alpha = \frac{L_{in}}{V_{in} T_s}$.

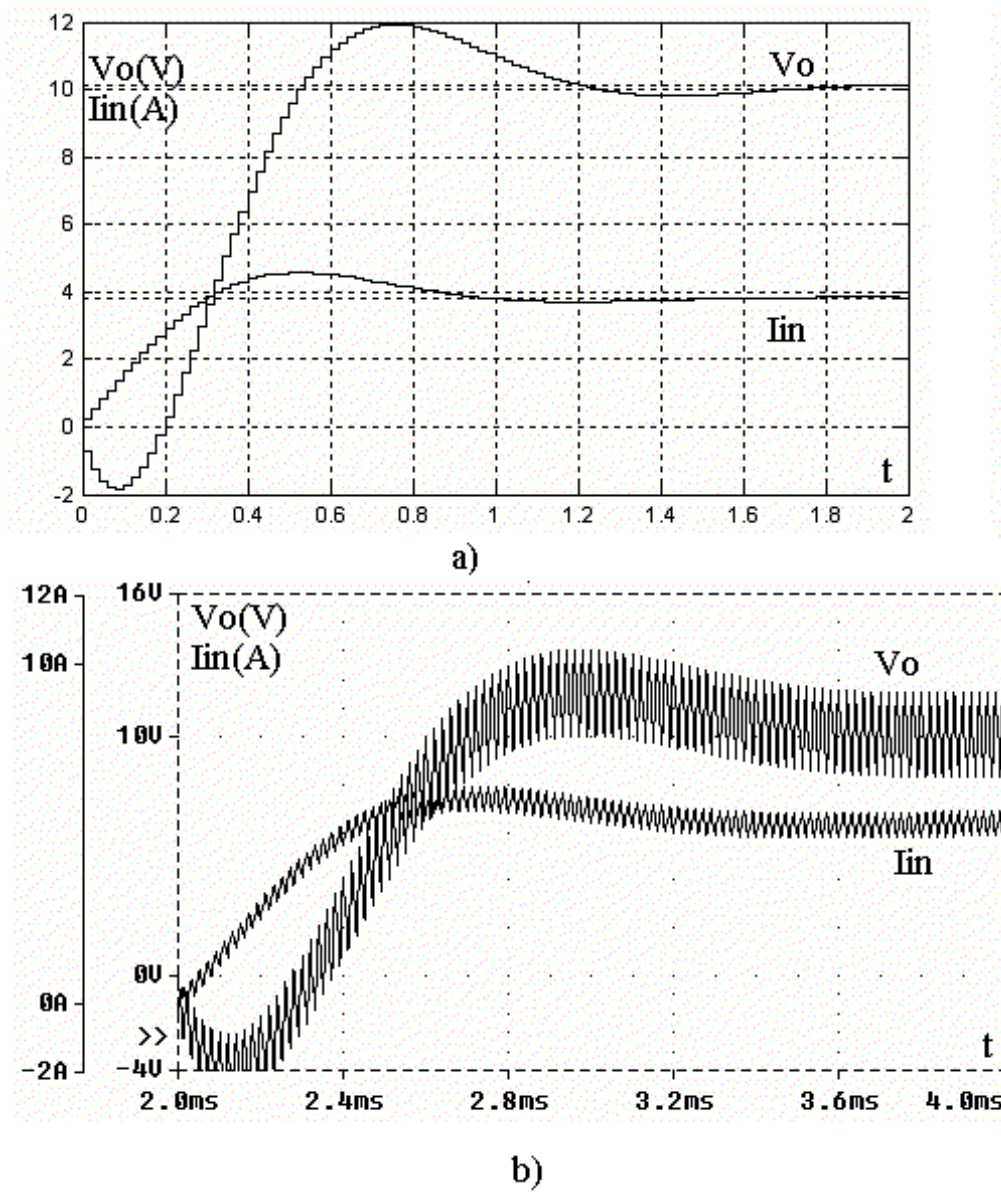


Figure 11: Simulation results of a transient process for the boost converter in an open loop system ($V_{in}=\text{const}$). a) Matlab-Simulink z-model, b) PSPICE simulation.

In general, the equation set in the z -region is similar to (26), i. e.,

$$\begin{aligned}\hat{i}_{in}(z) + a_V(z)\hat{v}_o(z) &= V_{oo}\hat{D}_C \frac{T_s}{L_{in}} \frac{z^2}{(z-1)^2}; \\ \hat{v}_o(z) &= -I_{Co}\hat{D}_C \frac{T_s}{C_o} \frac{ze^{-\Delta D}}{z-e^{-\Delta}} + \frac{D_1 T_s}{C_o} \hat{I}_C \frac{ze^{-\Delta D}}{z-e^{-\Delta}}.\end{aligned}\tag{29a}$$

Taking into account (28), one gets

$$\begin{aligned}-c_V(z)\hat{i}_{in}(z) + a_V(z)\hat{v}_o(z) &= \hat{I}_C \frac{V_{oo}}{V_{in}} \frac{z^2}{(z-1)^2}; \\ -c_i(z)\hat{i}_{in}(z) + \hat{v}_o(z) &= \hat{I}_C a_i(z) \frac{z}{z-1} - \hat{I}_C c_i(z) \frac{z}{z-1},\end{aligned}\tag{29b}$$

where

$$c_V(z) = 1 + \frac{z}{z-1} \frac{V_{oo}}{V_{in}}; \quad c_i(z) = \frac{L_{in} I_{Co}}{C_o V_{in}} \frac{ze^{-\Delta D}}{z-e^{-\Delta}}.$$

Based on the last set of equations in the continuous current mode, one gets

$$\begin{aligned}G_{ic}(z) &= \frac{d_{2i}z^2 + d_{1i}z}{c_2z^2 + c_1z + c_0}; \\ G_{vc}(z) &= \frac{d_{2v}z + d_{1v}e^{-\Delta D}}{c_2z^2 + c_1z + c_0},\end{aligned}\tag{30}$$

where

$$\begin{aligned}c_2 &= 1 + \frac{D_1 I_{co} T_s}{V_{in} C_o} + \frac{V_{oo}}{V_{in}}; \quad c_1 = -\frac{V_{oo}}{V_{in}} e^{-\Delta} + \frac{D_1 I_{co} T_s}{V_{in} C_o} e^{-2\Delta}; \quad c_0 = e^{-\Delta}; \\ d_{2i} &= \frac{V_{oo}}{V_{in}} - D_1 e^{-2\Delta D} \left(D_1 T_s^2 \frac{1}{L_{in} C_o} - \frac{T_s I_{co}}{C_o V_{in}} \right); \quad d_{1i} = -\frac{V_{oo}}{V_{in}}; \\ d_{2v} &= \frac{D_1 T_s}{C_o} \left(\frac{V_{oo}}{V_{in}} - 1 \right) e^{-\Delta D} + \frac{L_{in} I_{co}}{C_o V_{in}} e^{-\Delta D}; \quad d_{1v} = \frac{D_1 T_s}{C_o} e^{-\Delta D} - \frac{L_{in} I_{co}}{C_o V_{in}} e^{-\Delta D}.\end{aligned}$$

Fig. 12 shows the simulation results of the boost-converter in Simulink (Fig. 12,a) and PSPICE (Fig. 12,b) for the same values of parameters as in the previous cases for $I_{co} = 5A$; $\hat{I}_c = 1A$.

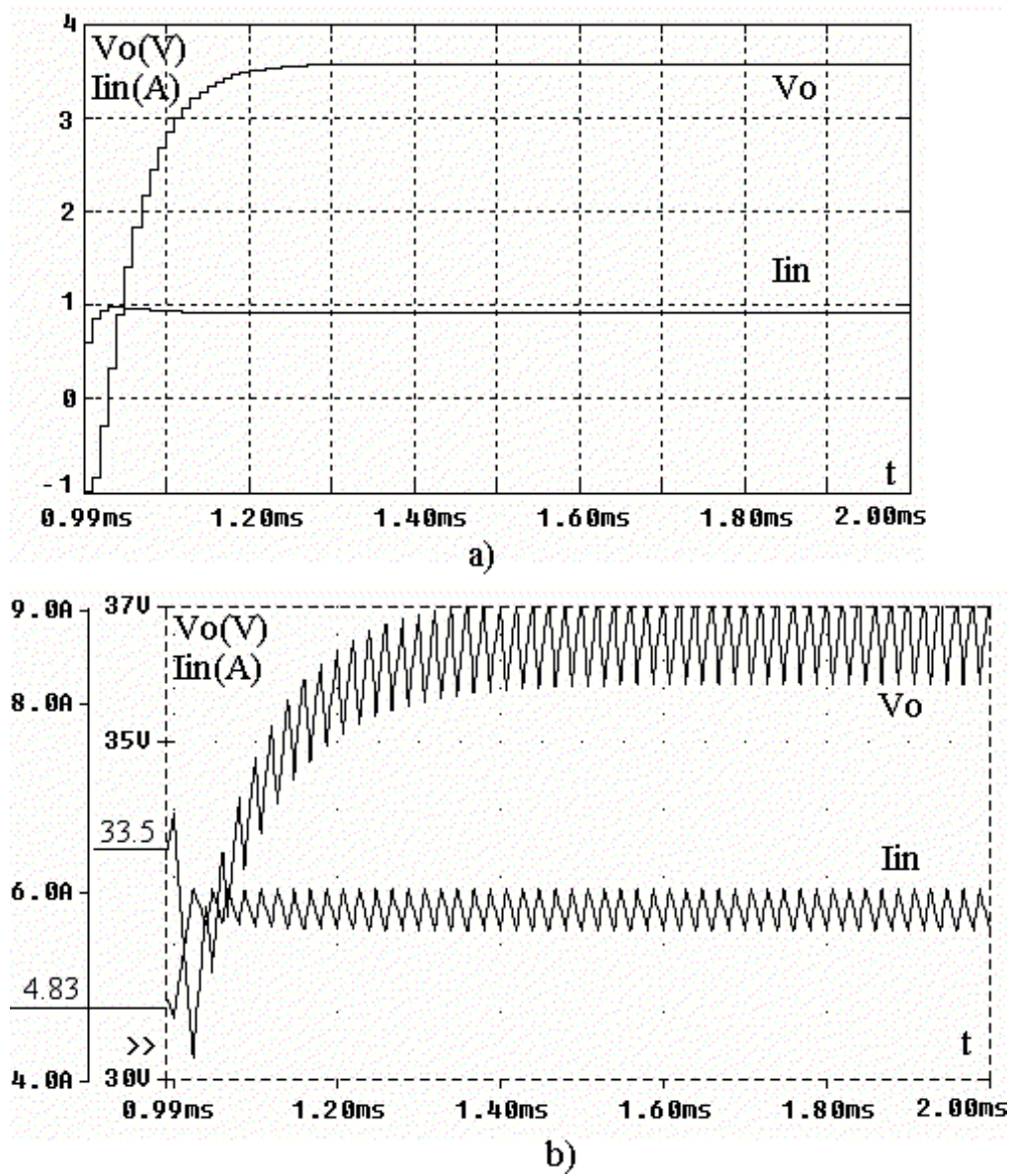


Figure 12: Simulation results of a transient process in CCM for the boost converter. a) Matlab-Simulink z-model, b) PSPICE simulation.

3.4 Closed loop system

In the closed loop system, the change of the duty cycle \hat{D}_k in the k -th period in (25b) is determined as

$$\hat{D}_k = \frac{\hat{v}_c F}{V_{ramp}},$$

where \hat{v}_c is obtained according to (11). The simultaneous changes in the input voltage V_{in} and duty cycle \hat{D}_k are taken into account by the system of equations (20) or (25b) where the right-hand part of a new system will be equal to the sum of terms in the right hand parts of these equations not containing variables $\hat{v}_{o.k}^*$ and $\hat{v}_{in.k}^*$.

Fig. 13a shows the results of simulation of the starting process of the boost-converter with zero initial conditions in the closed loop system in Matlab-Simulink. The circuit parameters correspond to those mentioned above, the feedback factor $k_o = 0.1$, and the time constant of the integral regulator $G(s) = \frac{1}{sT_C}$ is $T_C = 1250\mu s$. Calculations were performed in the s-model obtained on the basis of the equations (20) and (25b) for joint variations of the input and control signals. The results of PSPICE-modeling are given for comparison in Fig. 13b.

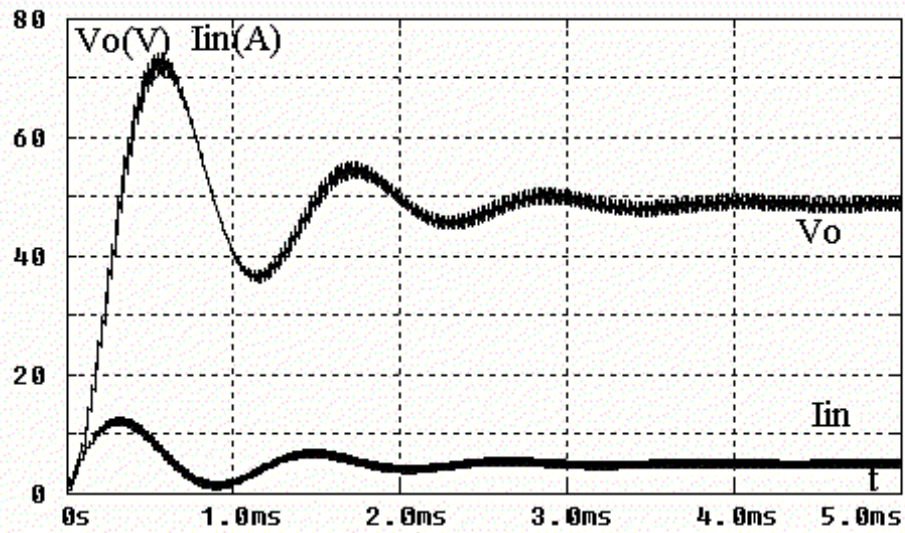
4 Experimental results

For checking the results of the theoretical analysis in Sections 2 and 3, a prototype of the circuit was built for: $V_{in} = 24V$; $L_o = 100\mu H$; $C_o = 5\mu F$; $R_o = 2.9\Omega$; $f = 50kHz$, transistor of the IRF-540 type for the switch and diodes MBR.

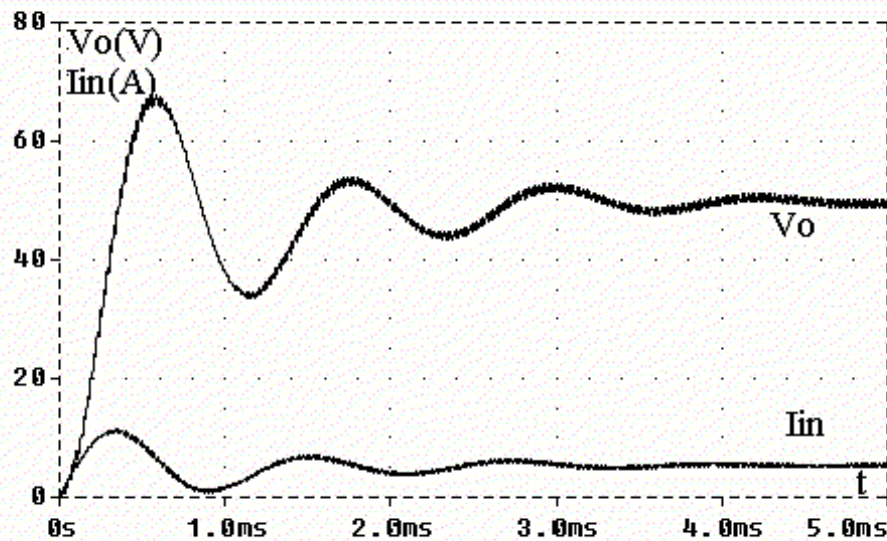
The transient process at switching on the converter for a constant voltage in the open loop system is shown in Fig. 14a. The same process in the closed loop system with an integrated regulator ($C = 0.036\mu F$, $R = 1k\Omega$) and gain $k_o = 0.25$ is shown in Fig. 14b. Fig. 14c shows the switch voltage in the process of period doubling at a transition of the buck-converter in an unstable mode ($C = 0.01\mu F$). The experimental results and theoretical analysis are in good agreement.

5 Conclusions

The discrete model in comparison with the continuous one provides more precise values of voltages and currents, especially at small inductances and



a)



b)

Figure 13: Simulation results of a step-up transient process for the boost converter in a closed loop system. a) Matlab-Simulink *s*-model, b) PSPICE simulation.

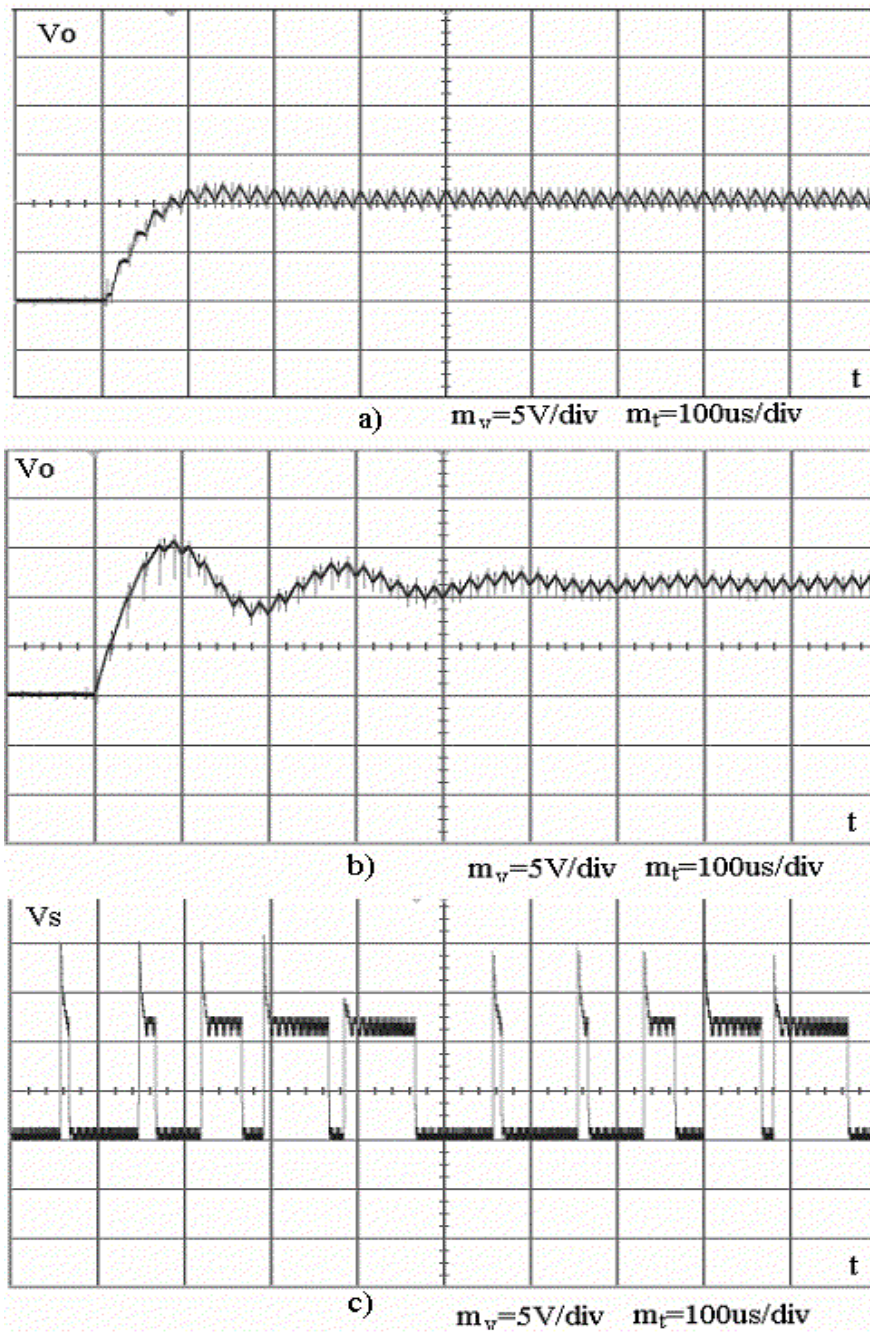


Figure 14: Experimental start-up output voltage for the buck converter. a) open loop system, b) closed loop system, c) closed loop system, unstable mode.

capacitances. The pulse model is more adequate at the analysis of the converter with digital control devices. The linearized continuous model essentially cannot give understanding of such important modes as period doubling and subsequent forming of chaotic modes. The pulse model keeps discrete character of the converter operation, therefore its transition to an unstable mode with appearing of period doubling are more logical for such a model.

References

- [1] R.D. Middlebrook and S. Cuk, *Advances in Switched-Mode Power Conversion*, vol. I, II and III (TESLACO, 1981).
- [2] D. Zhou, A. Pietkiewicz, and S. Cuk, Proc. Applied Power Electronics Conference and Exposition, APEC '95, 5-9 Mar., 1995, Dallas, TX, USA, p. 283 (1995).
- [3] Y. Berkovich and A. Ioinovici, IEEE Trans. on Circuits and Systems **47**, 860 (2000).
- [4] C.K. Tse, *Complex Behavior of Switching Power Converters*, p. 262 (CRC Press, Boca Raton, Fl., 2004).
- [5] C.-C. Fang, The 2001 IEEE International Symposium on Circuits and Systems, ISCAS'2001, 6-9 May, 2001, Sydney, Australia, p. III-731 (2001).